Studies on the Nitroreductase Prodrug-Activating System. Crystal Structures of Complexes with the Inhibitor Dicoumarol and Dinitrobenzamide Prodrugs and of the Enzyme Active Form

Eric Johansson,[†] Gary N. Parkinson,[†] William A. Denny,[‡] and Stephen Neidle*[,†]

Cancer Research UK Biomolecular Structure Group, The School of Pharmacy, University of London, 29-39 Brunswick Square, London WC1N 1AX, United Kingdom and Auckland Cancer Society Research Centre, School of Medical Sciences, The University of Auckland, Private Bag 92019, Auckland 1000, New Zealand

Received March 7, 2003

The *E. coli* nitroreductase enzyme (NTR) has been widely used in suicide gene therapy (GDEPT and ADEPT) applications as a activating enzyme for nitroaromatic prodrugs of the dinitrobenzamide class. NTR has been previously shown to be a homodimeric enzyme with two active sites. We present here the crystal structures of the reduced form of NTR and its complexes with the inhibitor dicoumarol and three dinitrobenzamide prodrugs. Comparison of the structures of the oxidized and reduced forms of the native enzyme shows that the principal structural changes occur in the FMN cofactor and indicate that the enzyme itself is a relatively rigid structure that primarily provides a rigid structural framework on which hydride transfer occurs. The aziridinyldinitrobenzamide prodrug CB 1954 binds in nonidentical ways in both of the two active sites of the homodimeric enzyme, employing both hydrophobic and (in active site B) a direct H-bond contact to the side chain of Lys14. In active site A the 2-nitro group stacks above the FMN, and in active site B the 4-nitro group does, explaining why reduction of either nitro group is observed. In contrast, the larger mustard group of the dinitrobenzamide mustard compound SN 23862 forces the prodrug to bind at both active sites with only the 2-nitro group able to participate in hydride transfer from the FMN, explaining why only the 2-hydroxylamine reduction product is observed. In each site, the nitro groups of the prodrug make direct H-bond contacts with the enzyme; in active Site A the 2-nitro to Ser40 and the 4-nitro to Asn71, while in active Site B the 2-nitro contacts the main chain nitrogen of Thr41 and the 4-nitro group the Lys14 side chain. The related amide-substituted mustard SN 27217 binds in a broadly similar fashion, but with the larger amide group substituent able to reach and contact the side chain of Arg107, further restricting the prodrug conformations in the binding site. The inhibitor dicoumarol appears to bind primarily by π-stacking interactions and hydrophobic contacts, with no conformational changes in the enzyme. One of the hydroxycoumarin subunits stacks above the plane of the FMN via π-overlap with the isoalloxazine ring, penetrating deep into the groove, with the other less well-defined. These studies suggest guidelines for further prodrug design. Steric bulk (e.g., mustard rather than aziridine) on the ring can limit the possible binding orientations, and the reducible nitro group must be located para to the mustard. Substitution on the carboxamide side chain still allows the prodrugs to bind, but also limits their orientation in the binding site. Finally, modulating substrate specificity by alteration of the structure of the enzyme rather than the prodrug might usefully focus on modifying the Phe124 residue and those surrounding it.

Introduction

The concept of 'bioreductive therapy' evolved separately in several fields, including cancer chemotherapy, solid tumor radiosensitization, and antimicrobials.[1] The technique relies on the enzymatic reduction of a nontoxic prodrug to a reduced form that is considerably more cytotoxic. Selectivity for tumor tissue is achieved in a number of different ways. One is the use of endogenous reductases that are inhibited by oxygen, or which initially metabolize the prodrug to a transient intermediate that can be back-scavenged by oxygen. Both of these approaches rely on the fact that solid tumors are distinguished from normal tissue by the presence of hypoxic regions, in which the prodrugs are activated.

Another approach is the use of reductase enzymes in 'suicide gene therapy'. Here an exogenous, oxygen-insensitive reductase enzyme is either conjugated directly to a tumor-specific delivery system such as an antibody (as in antibody-directed enzyme prodrug therapy; ADEPT), or the gene for the enzyme is incorporated into an appropriate tumor-specific vector and delivered to and expressed in tumor cells[2] (viral- or gene-directed enzyme prodrug therapy; VDEPT or GDEPT). Nitroreductase enzymes have a potential advantage in suicide gene therapy, since metabolism of an aromatic nitro group (Hammett $\sigma_p = 0.78$) to the corresponding hydroxylamine ($\sigma_p = -0.34$) results in a

* To whom correspondence should be addressed. Tel.: 44 207 753 5969, Fax: 44 207 753 5970, e-mail Stephen.neidle@ulsop.ac.uk.
[†] University of London.
[‡] The University of Auckland.

10.1021/jm030843b CCC: $25.00
Published on Web 08/07/2003

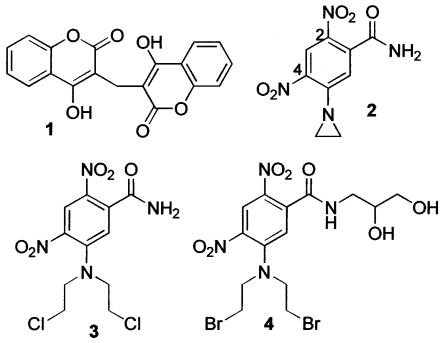

Figure 1. Formulas of drugs used in this study.

very large electronic change, providing an effective "switch" mechanism.

The most widely studied nitroreductase for GDEPT is the oxygen-insensitive enzyme from *E. coli* (the *nfsB* gene product; NTR[3]). This has the ability to reduce a wide range of nitro-containing compounds such as nitrofurazone (to the hydroxylamines) and quinones such as menadione (to the quinols). It is specifically inhibited by the irreversible inhibitor dicoumarol (Figure 1: **1**). The ability of NTR to reduce aromatic nitro groups to the corresponding hydroxylamine (and possibly amine) derivatives has been exploited for cancer chemotherapy mainly with the dinitrobenzamide class of prodrugs. In particular, the 5-aziridinyl-2,4-dinitrobenzamide CB1954 (**2**) has been well-studied as a prodrug for GDEPT with NTR.[4] This compound was initially shown to effect complete cures of Walker 256 rat carcinoma in vivo and was highly cytotoxic in some cell cultures.[5] This is due to its specific activation by rat DT-diaphorase[6] [DTD; NAD(P)H dehydrogenase (quinone)], via reduction of the 4-nitro group to the hydroxylamine, which after further activation gives a DNA interstrand cross-linking species.[7] Compound **2** was subsequently shown to be a much poorer substrate for human than rat DTD (K_{cat} = 0.64 min^{-1} and 4.1 min^{-1}, respectively), but a much better substrate for NTR[8] (K_{cat} = 360 min^{-1}). Thus, it has been widely studied as a prodrug for NTR/GDEPT[9] and a Phase I clinical trial in combination with adenovirus-delivered NTR is in progress.[10]

NTR uses FMN as a cofactor to mediate two-electron transfer reactions, which proceed via a ping pong Bi Bi mechanism. In the first step, two electrons are transferred from NAD(P)H to the FMN. Then the substrate (in this case the prodrug) enters the active site through one of two quite narrow channels (A and B) and is reduced to the hydroxylamine derivative via the unstable nitroso intermediate, a total of two two-electron transfers of which NTR need only be directly involved with one. In the case of compound **2**, NTR can reduce either the 2- or the 4-nitro group (but not both). Acetylthioesters then convert the hydroxylamines to the *N*-acetoxy derivatives, of which only the 4-*N*-acetoxy results in highly cytotoxic DNA cross-linking.

There is interest in carrying out variations on the dinitrobenzamide scaffold of compound **2** to find analogues with superior potency and selectivity toward NTR-transfected tumor cells. The dinitrobenzamide mustard derivative, SN23862 (Figure 1: **3**) is also a substrate for NTR, with a higher turnover (K_{cat} = 1580 min^{-1}) than compound **2**.[11] In addition, it is not a substrate for DT diaphorase,[12] which may increase its selectivity in NTR/GDEPT. It is also substantially more lipophilic than compound **2** (measured log *P* values of 1.54 and 0.14, respectively) and has a correspondingly greater bystander effect.[13]

In contrast to compound **2**, the reduction of **3** by NTR is regiospecific, leading only to the 2-hydroxylamine derivative, and, after another two-electron transfer, the amine. Either of these two reductions are sufficient to fully activate the mustard group to a DNA cross-linking agent. The fact that only the 2-nitro group is reduced is somewhat surprising on thermodynamic grounds, as radiolytic experiments have shown that the 4-nitro group is the more electron-affinic of the two.[14]

A wide range of compounds based on the dinitrobenzamide motif of compounds **2** and **3** have been synthesized and examined as prodrug candidates for the NTR system.[15] However, rationalizing these modifications with the wealth of biochemical and biophysical data available has so far been hampered by the lack of detailed structural information. The elucidation of the structure of the native NTR enzyme in our laboratory[16] and, subsequently, elsewhere, in complex with nicotinic acid,[17] has shed light on many aspects of the enzyme itself and its mechanism. The structure of the active site has allowed informed speculation on how prodrugs would interact, and some molecular modeling docking has been carried out using this crystal structure and compound **2**.[16] However, direct structural information on how prodrugs interact with the enzyme is notably lacking, as is the structure of the enzyme in its reduced (active) form. Such data would prove invaluable in defining structure−activity relationships (SAR) for prodrugs binding to NTR that would allow rational design of superior candidates. This information may also make it possible to carry out modifications on the enzyme itself, to improve its characteristics as an activator of dinitrobenzamide prodrugs.

The nature of the Ping Pong Bi Bi catalytic mechanism of NTR raises problems in addressing the way in which the prodrugs interact with it. A complex of the reduced, active enzyme with a bound prodrug will not exist for long enough to allow crystallization and X-ray data collection. An important assumption must therefore be made, that the enzyme does not undergo significant conformational changes on reduction that would have consequences for prodrug binding in the active site. This assumption implies that the enzyme merely provides a scaffold for electron exchange to occur, and that the changes in binding affinities during catalysis are due to electronic changes in the FMN prosthetic group as it shifts between redox states. However, even before any structural studies were carried out, this assumption was supported by several observations. First, the structure of the native enzyme reveals that access to the binding pockets through Channel A does not require any conformational changes to take place. Second, the active site appears to be quite rigid, both in terms of the main and side chain atoms.

In this paper we report on the crystal structures of the reduced form of NTR, both as native enzyme and complexed with the inhibitor dicoumarol (compound **1**) and the prodrugs compounds **2**, **3**, and **4** (SN27217:

Table 1. RMS Deviation Analysis of Main-Chain (MC) and Side-Chain (SC) Residues within 10 Å of the FMN Molecules in the Structures Reported Here, Compared with Both Native and Reduced NTR Structures

		native				reduced			
		MC	SC	MC	SC	MC	SC	MC	SC
native	MC								
	SC								
	MC								
	SC								
reduced	MC	0.19							
	SC		0.28						
	MC			0.22					
	SC				0.44				
compound **2**	MC	0.18				0.14			
	SC		0.26				0.26		
	MC			0.6				0.1	
	SC				0.31				0.44
compound **3**	MC	0.16				0.14			
	SC		0.24				0.25		
	MC			0.17				0.2	
	SC				0.3				0.4
compound **4**	MC	0.17				0.27			
	SC		0.28				0.51		
	MC			0.2				0.18	
	SC				0.38				0.44
compound **1**	MC	0.18				0.15			
	SC		0.31				0.29		
	MC			0.18				0.23	
	SC				0.34				0.43

Figure 1). The reduced structure supports the assumptions made above and shows that the main changes on reduction occur in the FMN. The structures of the prodrug complexes provide explanations for some of the biological observations made. In particular, they provide the first structural explanation as to the observed regiospecificity of activation.

Results and Discussion

Structure of Reduced NTR. The reduced FMN structure is closely isomorphous with the native NTR structure (PDB 1DS7), the overall RMS deviation for the native and reduced structures was 0.19, 0.28, 0.22, and 0.44 Å for side and main chain in active site A and B, respectively, for residues within 10 Å of the active site (Table 1), indicating that no major structural changes occur in the enzyme itself on reduction. Careful examination of the electron density corresponding to the prosthetic groups indicated that both FMN molecules seemed to have adopted the characteristic butterfly conformation of the reduced forms, though in the FMN of Active Site B, the buckling was more pronounced. The angles between the N5 and N10 atoms were 149° and 139° in active sites A and B, respectively.

An important question is whether the reduced FMN molecule fully satisfies its hydrogen bonding capability and what changes take place on reduction. The N5 of the flavin is known to often be within hydrogen-bonding distance of a hydrogen bond donor, usually a backbone or side chain nitrogen atom. In the case of the N5 in NTR, the hydrogen bond donor appears to be the main chain amide nitrogen of Glu165. On reduction, the N5 atom of FMN becomes protonated, and the hydrogen bond interaction observed in other nonreduced NTR structures between this atom and the main chain nitrogen atom of Glu165 cannot occur. In active site B, the Glu165−N5 distance in the reduced structure is 3.54 Å and the Glu165−N5−N10 angle is 139° so that there is no longer a hydrogen bond interaction at this position. Instead the Gly166 is better positioned to contact this atom. The question is therefore whether movement in the Glu165 residue or the prosthetic group accounts for this. The RMS deviation between Glu165 in the native and reduced structures is small and probably insignificant given the resolution of the structure, and furthermore the most striking difference seems to be in the conformation of the prosthetic groups. This indicates that the FMN is responsible for the change around this locus. Although the exact role of the hydrogen bond at this locus has not been determined, it has been shown to be involved in modifying/fine-tuning the redox potential of the FMN and is therefore important for allowing the progression of the reaction mechanism.[17]

Another feature conserved throughout the flavoprotein family is the N1−C2═O2 locus of the flavin, which is always in contact (<3.5 Å) with a positively charged motif. In NTR, this region is in contact with two positively charged lysine residues, Lys14 and Lys74, which tend to hydrogen bond to the O2. Figure 2a shows the distances around this locus. The carboxyl O2 is within hydrogen bonding distance to the nitrogen atoms of Lys14 and Lys74 in both the native and active site B of the reduced structures. Though the FMN in active site A only contacts Lys14, the important feature at this point is that the N1−C2═O2 locus is always in contact with at least one positively charged residue as shown in Figure 2b. This is known both to favor flavin binding and to modulate its redox potential, and we speculate that this proximity might serve to stabilize the transient negative charge that develops on the N1 atom as the FMN is reduced.[18]

Complexes with Prodrugs. All the prodrug complexes described in this study were isomorphous with that of the native structure of the enzyme, indicating that no major structural changes take place on prodrug binding. This was further reinforced by the results of RMS deviation analysis (see Table 1), which show that the differences between the various structures are small. Any differences were limited to the local conformations of some side chains around the active sites but, as will be seen, there was little consistency in these throughout these structures nor of the other crystal structures of NTR solved to date. The FMN cofactors are well defined throughout the structures of this study and tend to deviate slightly from planarity with a buckling across the N5−N1 locus as observed in previously determined NTR structures.[16,17] However, as expected, the degree of buckling is not indicative of the enzymes being in their reduced state.

Compound 2: Binding Orientation. Both of the enzyme active sites have well-defined electron density corresponding to the prodrug molecules (Figure 3a). Fitting the prodrugs into this electron density revealed that in both active sites the prodrug molecules stack above the plane of the FMN with a distance of about 3.5 Å and are held to the flavin by π-overlap of the nitro group with the isoalloxazine ring. However, as shown in Figure 3b, the two prodrug molecules in the active sites are in different orientations and therefore nonidentical environments. In active site A, the prodrug

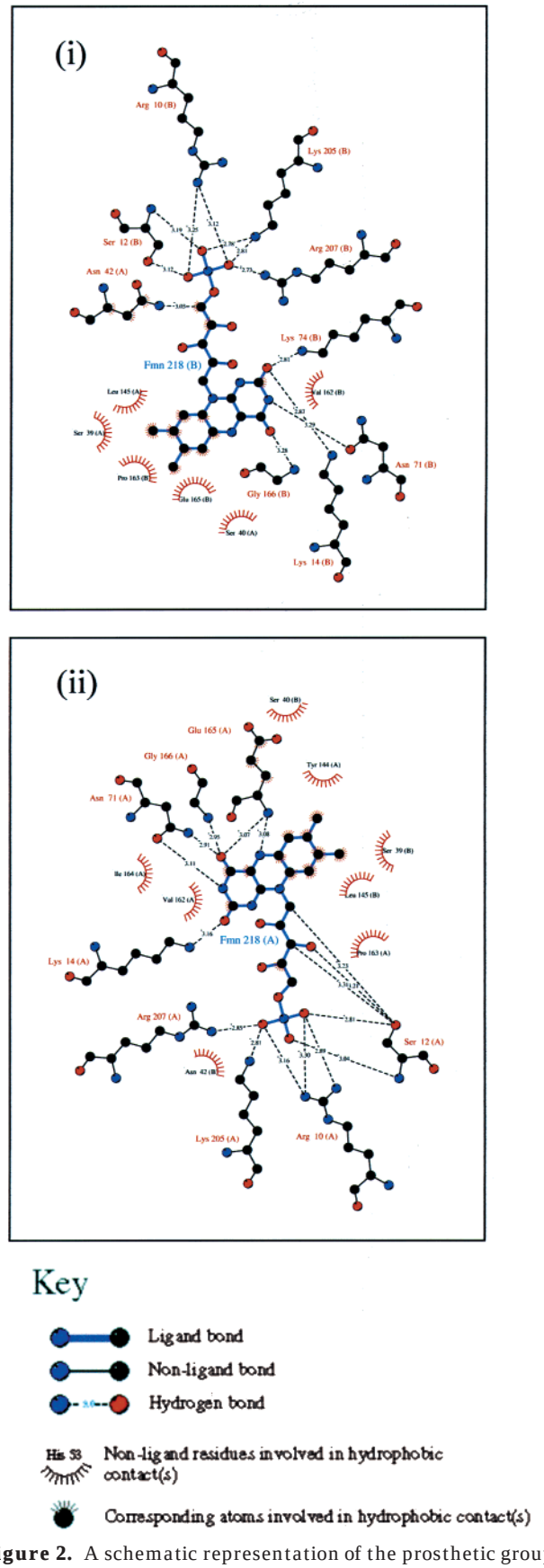

Figure 2. A schematic representation of the prosthetic group interactions of the FMN molecules in Active Sites (i) A and (ii) B.

molecule is oriented so that the 2-nitro group faces into the binding site, stacking above the FMN cofactor with the aziridine ring facing outward. In this orientation, the prodrug buries 355.7 Å^3 of the solvent-accessible area. In active site B, on the other hand, the prodrug molecule is oriented so that it is the 4-nitro group that stacks above the cofactor, with the aziridine ring pointing into Channel B toward the Phe124 residue, burying 514.6 Å^3 of the solvent-accessible volume. Interestingly, the orientation of the prodrugs relative to the FMN molecules is not exactly linear. Instead, they bind at an angle to the plane of the FMN. This is in accord with results from modeling studies[16] and also with structural studies on quinone compounds binding to DT-diaphorase.[18]

Compound 2: Interactions with NTR. Stacking interactions with the flavin molecule are important for the binding of the prodrugs, but are not the only forces that hold them in place. Due to the two different binding orientations of the molecules of compound **2** in the active sites, the interactions that they make with the surrounding features such as amino acid residues and water molecules are nonidentical. Figure 3c shows representations of the surrounding amino acid residues and solvent molecules of importance for prodrug binding in the two sites. The positions of the solvent atoms surrounding the prodrugs in the active sites are quite well conserved relative to each other. As illustrated in Figure 3d, the network of waters in active site A, made up of O97 (Tip106), O125 (Tip139), O5 and O38, is mirrored in the other active site by O45, O93 (Tip182), O48, O43. There are no direct contacts between compound **2** in active site A and the enzyme, though there are several solvent-mediated ones. The amide group of the prodrug in active site A is within hydrogen bonded distance of two waters, O125 (Tip139) and O97 (Tip106), which serve as a bridge to the Glu102/Asn117 and Arg121 of the enzyme, respectively. The ligand also makes hydrophobic contacts to Phe 124.

In active site B, the 2-nitro group forms a hydrogen-bonded contact to O93/Tip182, which in turn interacts with Asn117 and Glu102. It also forms a direct hydrogen-bonded contact to the side chain of Lys14, which also contacts the amide oxygen. The 4-nitro group forms a direct contact to the main chain amide of Thr41. The aziridine ring makes hydrophobic contacts to both the Phe124 and Phe70, which in this site is in an alternative conformation to that observed previously and faces the ribityl portion of the FMN partially shielding the active site. Therefore, only compound **2** in active site B is involved in any direct hydrogen bond to enzyme residues, which may account for the *B*-factors of the prodrug in this site being slightly lower (53.4 Å^2 vs 50.8 Å^2).

Compound 3: Binding Orientation. Examination of electron density maps in the active sites revealed well-defined regions of density above the planes of the FMN molecules in both active sites, clearly showing the positions of the mustard and amide groups (Figure 4a). The orientations of the molecules of compound **3**, which contrary to compound **2** does not have a pseudo 2-fold symmetry axis in regards to the shape of its electron density cloud, were limited in the active sites in terms of the positioning of the nitro groups. However, the drug molecules are rotated so that the amide groups face different sides in the two active sites, away and toward Channel B in Active Sites A and B, respectively. Fitting the structure of **2** into the electron density in an

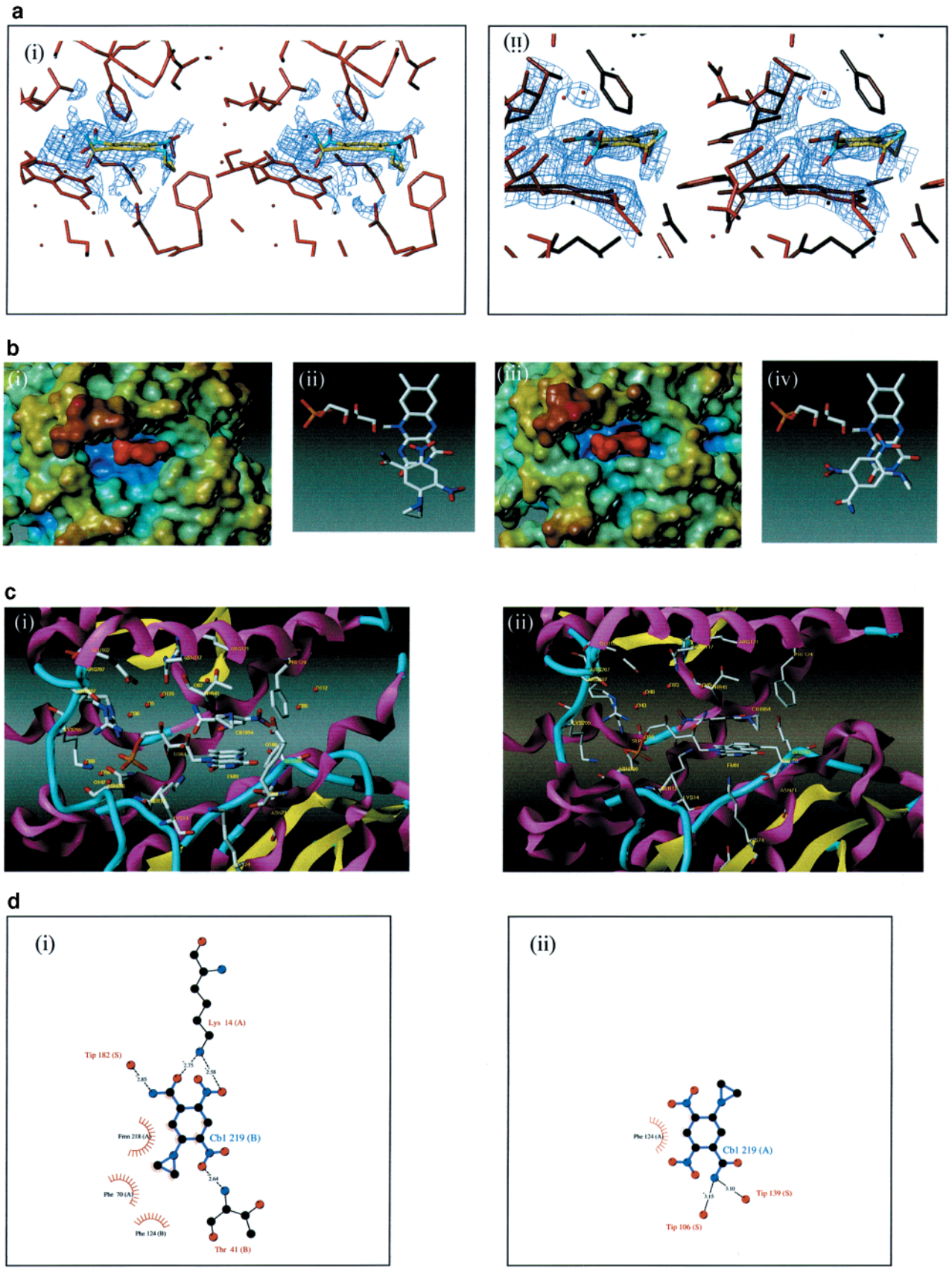

Figure 3. The structure of the NTR complex with compound **2**, showing (a) a $2F_o - F_c$ electron density map contoured at 0.5 σ levels around the prodrug molecule in active sites (i) A and (ii) B. (b) (i) A Connelly solvent-accessible surface representation and (ii) a view onto the prodrug stacked above the FMN, for active site A (i and ii) and active site B (iii and iv). (c) Ribbon and (d) a schematic representation of the interactions made by the prodrug molecules with surrounding solvent and amino acid residues in active sites (i) A and (ii) B.

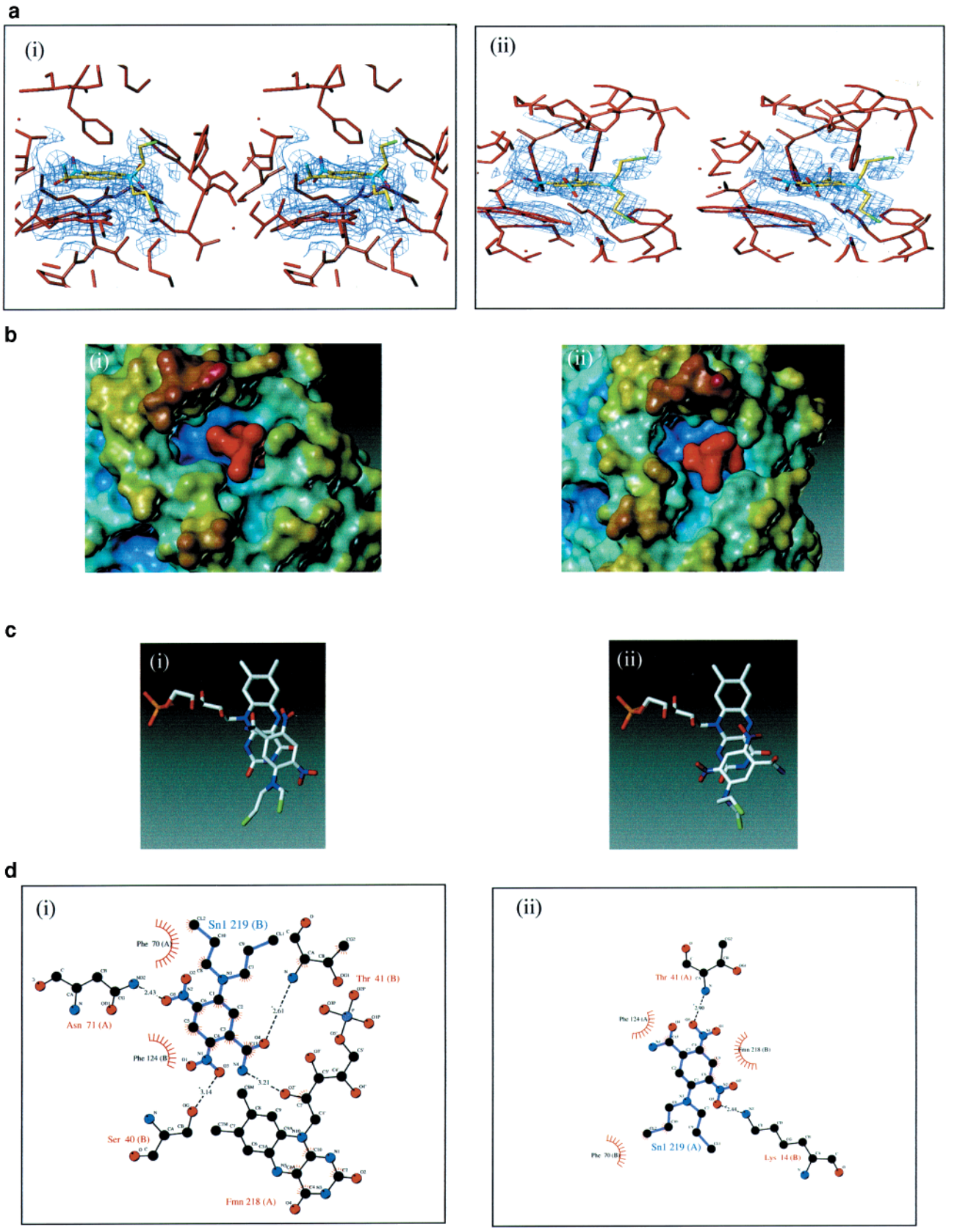

Figure 4. The structure of the NTR complex with compound **3** showing for active sites A (i) and B (ii) (a) a $2F_o - F_c$ electron density map contoured at 0.5 σ levels around the prodrug molecule and in, (b) a Connelly solvent-accessible surface representation, (c) a view onto the prodrug stacked above the FMN in Active Site B, and (d) a schematic representation of the interactions made by the prodrug molecules with surrounding amino acid residues in active sites A and B.

unambiguous manner required careful examination of the surrounding environment. However, the presence of the mustard group of **3** and, in particular, the high scattering power of the chlorine atoms, make the orientations, shown in Figure 4b,c the only possible ones.

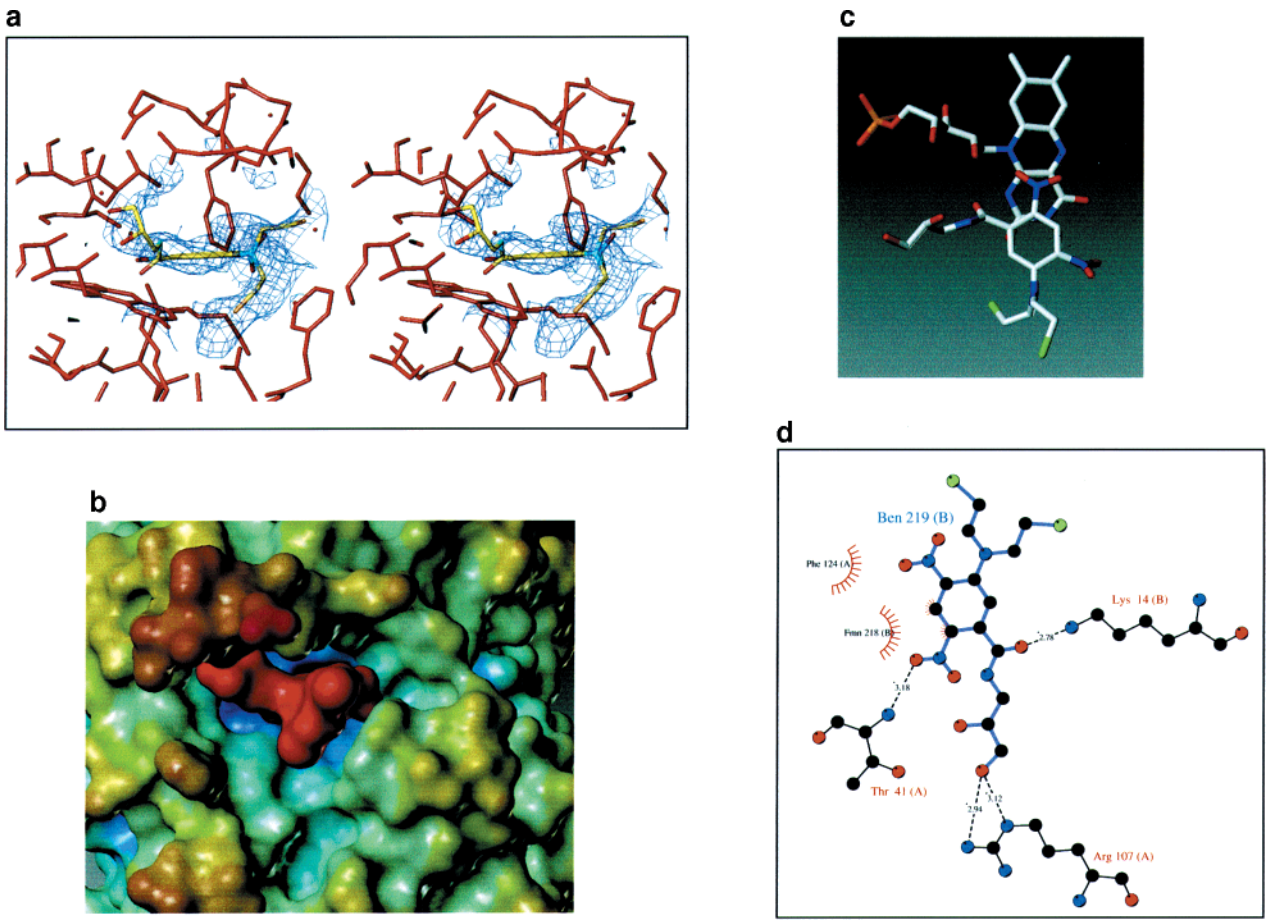

Figure 5. The structure of the NTR complex with compound **4** showing (a) a $2F_o - F_c$ electron density map contoured at 0.5 σ levels around the molecule, (b) a Connelly solvent-accessible surface representation, (c) a view onto the prodrug stacked above the FMN in active site B, and (d) a schematic representation of the interactions with surrounding amino acid residues.

Compound **3** stacks above the FMN with a distance of about 3.5 Å, allowing π-overlap with the flavin isoalloxazine ring. Again, the orientation of the prodrug relative to the FMN deviates from planarity. The 2-nitro groups are positioned in such a way that they would be able to participate in hydride transfer with the reduced prosthetic group, as is further illustrated by Figure 4c. The binding of compound **3** excluded 636.3 Å^3 and 596.5 Å^3 of the solvent-accessible volume in Active Sites A and B, respectively, which, as expected from the larger mustard group, is more than that of the binding of **2**. Figure 4d shows a schematic representation of the molecules of **3** and their hydrogen bond and hydrophobic interactions to enzyme residues in the two active sites. In Active Site A, the 2-nitro group makes a direct contact to Ser40, whereas the 4-nitro group contacts Asn71. The amide group makes two direct contacts, one from the oxygen to Thr41 and another from the nitrogen to the FMN. In Active Site B, the 2-nitro group makes a direct contact to the main chain nitrogen of Thr41 and the 4-nitro group contacts the Lys14 side chain. Interestingly, no solvent-mediated contacts were observed in this structure. The Phe70 residue is in an alternative conformation to that of the native structure in Active Site A and also to that of Active Site B in the structure with **2**. This serves to illustrate the mobility of this residue and the little correlation that exist between the crystal structures of NTR solved to date in terms of this parameter.

Compound 4: Binding Orientation. Contrary to the situation with compounds **2** and **3**, a unique binding mode was observed for compound **4**, with the 2-nitro group stacked over the FMN and the amide group facing the ribityl portion of the FMN (Figure 5a). The larger amide group substituent prevents the prodrug from being able to rotate and face Channel B without steric clashing, notably with Phe124. The binding of **4** excludes a larger volume (734.4 Å^3) than the other two prodrug molecules reported here and thus appears to have a more intimate fit to the active site. This is further illustrated by Figure 5b,c, which shows how compound **4**, with its longer amide substituent group, complements the shape of the active site.

Compound 4: Interactions with NTR. The contacts made by **4** to surrounding enzyme and solvent residues are shown in Figure 5d. The 2-nitro group of this prodrug contacts the main chain nitrogen of Thr41, as was observed in Active Site B of the structure with compound **3**. The conformation of the side chain of Lys14 differs slightly from that of the structures discussed so far so that it does not contact the FMN but instead forms a direct hydrogen bond to the amide group oxygen of the prodrug. The longer substituent on the amide group also allows the molecule of **4** to reach and contact the side chain of Arg107. The average *B*-factor of the prodrug was 53.4 Å^2.

Dicoumarol: Binding Orientation. The family of flavoproteins of which NTR is a member are all inhib-

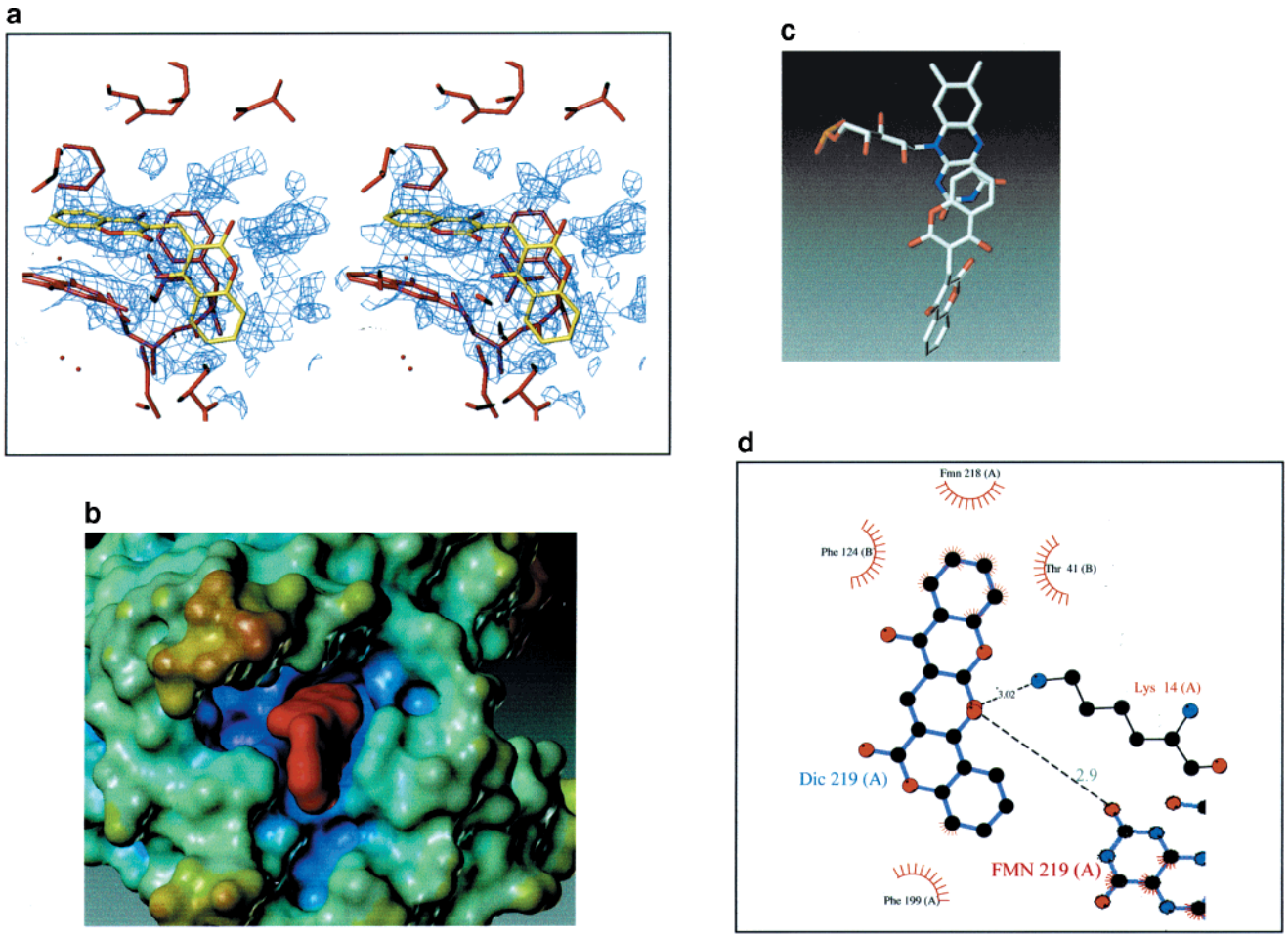

Figure 6. The structure of the NTR complex with compound **1** showing (a) a $2F_o - F_c$ electron density map contoured at 0.5 σ levels around the molecule, (b) a Connelly solvent-accessible surface representation, (c) a view onto the prodrug stacked above the FMN in active site B, and (d) a schematic representation of the interactions with surrounding amino acid residues.

ited specifically and irreversibly by dicoumarol, which is a competitive inhibitor with respect to the cosubstrate, NADH. Compound **1**), comprises two 4-hydroxycoumarins linked in a pseudosymmetrical manner by a carbon bridge. As in the crystal structure of the enzyme in complex with **4**, the electron density maps were only good enough to allow the confident fitting of the inhibitor molecule in one active site, A. Figure 6a shows a Connelly solvent-accessible surface representation and a top-view of **1** bound in the NTR active site. One of the hydroxycoumarin subunits stacks above the plane of the FMN and is held there by π-overlap with the isoalloxazine ring, penetrating deep into the groove. This binding mode has been corroborated by other crystal structures of **1** bound to FRase I, as well as by NMR studies.[19] This molecule is well buried with only the region toward the ribityl portion of the FMN not occupied by amino acid residues. Consequently, only one molecule can bind in the active site at any one time, which is consistent with the Ping Pong Bi Bi mechanism.

The second hydroxycoumarin subunit binds outward toward Channel A in a pseudoperpendicular way to the other subunit, so that the torsion angle between the two is 67°. The electron density (shown in Figure 6c) is not as well defined for this second subunit. This is probably due to its ability to adopt several conformations, as it is not held down by stacking interactions as is the other subunit. It was, however, not possible to justify any other position for the subunit on the basis of electron density though examination of Figure 6c shows that it should be able to rotate in respect to the stacked subunit and bind into Channel B. Therefore, the position shown is, at least in this structure, the predominant one, probably due to the hydrogen bond interaction formed between the hydroxyl group of the inhibitor and the carboxyl O2 of the FMN.

Compound 1: Interactions with NTR. This compound does not form significant direct contacts with any enzyme residues, with the notable exception of a hydrogen bond between the terminal nitrogen of Lys14 and the keto oxygen of the stacked hydroxycoumarin subunit. This suggests that π-stacking interactions are primarily responsible for stabilizing its binding. As shown in Figure 6d, compound **1** also makes several hydrophobic contacts to enzyme residues. These observations are in accordance with results from other structural studies on **1**.[19] It has an ideal chemical scaffold to enable it to stack above other conjugated ring systems such as FMN. The absence of any large substituents attached to the hydroxycoumarin subunit enable it to stack without causing steric clashes with either the FMN ribotide moiety or other enzyme residues. This feature accounts for its ability to inhibit such a wide range of flavoproteins.

This crystal structure reveals that no conformational changes are required in order to accommodate the inhibitor. This was not the case in the cocrystal structure of FRase I with the same inhibitor, in which the presence of the first hydroxycoumarin ring causes the Phe124 residue to move and the second ring causes movement of surrounding enzyme residues. Interestingly, in FRase I the conformation around this locus was poorly defined unless in the presence of inhibitor.[19] The native NTR structure, on the other hand, had a well-defined conformation in this region even in the native structure.[16] It thus appears that there is some difference in the behavior of these regions when confronted with ligands. It is tempting to speculate that this could account for differences observed in substrate specificity between the two enzymes, particularly given that NTR contains a two amino acid addition between residues 119 and 124 as compared to the FRase I. It therefore follows that site-directed mutagenesis in this region might provide a way of altering the substrate specificity of NTR to try to enhance its prodrug-activating characteristics.

Conclusions

Mechanism of Reduction. The NTR prodrug-activating system is a complicated one to address by crystallographic or any other structural means, due to the particular features of its reaction mechanism. At the same time, obtaining this type of information is highly desirable, as it would shed light on the way in which the enzyme carries out the function that makes it such an attractive candidate to use in prodrug therapy. The solution of the crystal structure of the native oxidized form of NTR[16,20] has shed some light, in structural terms, on how the enzyme works. It provided the first opportunity to examine the active site and served to explain why catalysis occurs by the Ping Pong Bi Bi mechanism. It was also possible to speculate where in the active site the cosubstrates, prodrugs, and inhibitors known to interact with the enzyme would bind and how they would interact. Importantly, examination of the residues around this area indicated that it was a relatively rigid structure, both in terms of side chain and, particularly, main chain conformations. This suggests that the enzyme merely provides a rigid structural framework, a stage, on which the hydride transfer and obligatory two-electron reduction reactions can occur. Furthermore, these reactions appear to be mediated by changes in the FMN prosthetic groups as they undergo redox cycling and not by changes in the structure of the enzyme itself. Therefore, soaking prodrugs into crystals of the oxidized form of the enzyme should provide valuable information on prodrug binding and interaction. The structure of the enzyme in its reduced form reported here supports this, showing that most of the changes were indeed observed in the structure of the prosthetic groups and not in enzyme itself.

Drug Orientation and Bioreductive Activation. The cocrystal structure of the prodrug compound **2** provides a structure-based explanation as to why NTR generates equal amounts of the 2- and 4-hydroxylamines. In active site A, the prodrug binds in such a way that the 2-nitro group is able to participate in hydride transfer with the FMN, leading to the less cytotoxic 2-hydroxylamine. In the other active site, the prodrug binds in an alternative orientation in which only the 4-nitro group can gain access to the prosthetic group. This binding mode, after further reduction and activation by thioesters, leads to the highly toxic, DNA cross-linking derivative reduced at the 4-position.

Compound **2** is thus relatively inefficient as a prodrug candidate for use in combination with NTR, in that two products are obtained in equal amounts, only one of which is highly cytotoxic. Modifications to the prodrug that bestow a definite orientation, so that only the 4-reduced derivative was formed, would increase the efficiency of the system. Compound **3** contains one such modification, with the bulky mustard group instead of the aziridine at the 5-position limiting the binding orientation to one in which only the 2-nitro group can stack above the FMN. This structure thus provides a plausible explanation as to why the action of NTR on **3** gives a unique species reduced at the 2-position, despite radiolytic experiments showing that the 4-nitro group has the higher electron affinity of the two.[21] The present study shows that structural, not electronic, factors are important for this regiospecificity and illustrates the importance of obtaining high-quality structural data in order to elucidate the function and mechanism of systems such as these.

The complex of nitroreductase with compound **4** again shows the consequence of having a bulky mustard group in terms of the regiospecificity of activation. As was the case for compound **3**, binding of the prodrug is limited to an orientation in which the 2-nitro group comes into contact with the FMN. The shape of the prodrug, with its larger carboxamide side chain, is more complementary to the shape of the active site and excludes more surface area than does the binding of **2** and **3**. At the same time, the relative orientation of the mustard and amide moieties seem to prevent the prodrug from rotating about its own axis to allow the amide group to face Channel B, as it would clash with the enzyme, particularly Phe124. The orientation of the prodrug in this crystal structure is therefore the only one possible, both in terms of the positioning of the 2-nitro group and that of the amide and 4-nitro groups. This probably goes some way to explain why analogues with substituents on the carboxamide side chain retain high activity with nitroreductase.[15]

Implications for Prodrug Design. In terms of altering prodrug structure to maximize the interaction with NTR, the information from the crystal structures in this study can be used to define certain rules. First, it is possible to use steric bulk at one position on the ring to limit the possible binding orientations. Mustard groups, such as that of compound **3**, are sufficiently large to achieve this, and at the same time directly result in DNA cross-linking species on activation. Second, the position of the trigger (the reducible nitro group) in relation to this bulky mustard is critical. These two substituents must be located para to each other in order for the nitro group to gain access to the FMN. Third, the crystal structure of the complex with **4** shows that substitution on the carboxamide side chain still allows the prodrugs to bind, but limits their orientations. Thus only the mustard, the carboxamide, and the

Table 2. Crystallographic Data[a]

structure	reduced	compd **2**	compd **3**	compd **4**	compd **1**
space group			$P4_12_12$		
unit cell parameters					
a (Å)	56.97	57.56	57.69	57.34	57.67
b (Å)	56.97	57.56	57.69	57.34	57.67
c (Å)	265.65	266.13	266.67	264.75	266.72
data collection					
max. resolution (Å)	2.5	2.0	2.0	2.49	2.0
no. of reflections	167692	31534	364175	166583	31904
no. of unique reflections	15515	28476	31642	15216	22217
completeness	96.2	90.5	73.8	83.3	70
	(89.2)	(96.8)	(70.9)	(78)	(82.7)
R_{merge} (%)	8.5	6.4	6.7	5.0	4.8
	36.9	(20.1)		11.9	(9.7)
refinement					
resolution range (Å)	20−2.5	20−2.0	20−2.0	2.0−2.5	20−2.0
	(2.7−2.5)	(2.1−2.0)	(2−2.13)	(2.66−2.5)	(2.13−2.0)
no. reflections used	15089	28431	23282	15016	22194
	(1986)	(4438)	(3437)	(2095)	(3833)
no. reflections used (R_{free})	151	2814	1373	1184	2204
sigma cutoff (*F*)	0.0	0.0	0.0	0.0	0.0
average isotropic *B* factor		29.28	27.8	27.8	21.2
no. atoms refined					
enzyme/B factor (Å^2)	3432	3432	3432	3414	3424
	39.7	29.2		27.8	
ligand/B factor (Å^2)	NA	36	44	27	25
			51.6	46.4	51.3
water	97	192	185	232	235
R_{all} (%)	20.4	22.2	23.1	21.4	22.5
	27.2	(24.3)	(25.3)	(28.0)	(24.7)
R_{free} (%)	28.9	26.3	28.6	26.4	27
	23.0	(28.3)	(31.9)	(31.4)	(30.5)
RMS deviations from ideal geometry					
bond (Å)	0.012	0.006	0.035	0.012	0.012
angle (deg)	1.23	0.8	1.16	1.4	1.2
dihedral (deg)	24.6	23.4	24.7	24.8	24.6
improper (deg)	1.19	0.99	1.68	1.54	1.43
PDB accession number	1005	1IDT	1006	100N	100Q

[a] Numbers in brackets refer to highest resolution shell. $R_{all} = [\Sigma|F_o(hkl) - F_c(hkl)|]/F_o(hkl)$. $R_{merge} = [\Sigma I_i(hkl) - <I(hkl)>]\Sigma I_i(hkl)$.

nitro group to be activated (2-nitro), properly positioned relative to each other, appear necessary to ensure specificity of activation. This means that, for the mustards, three other positions on the benzamide ring (and the carboxamide itself) are available to modulate other aspects of the prodrugs, such as nitro group reduction potential, solubility, lipophilicity, etc. This is demonstrated in a recent study[14] where the 4-nitro group of compound **3** was replaced by SO_2Me, with some retention of nitroreductase activity.

During the course of these studies, it has also become apparent that the Phe124 residue is important for nitroreductase specificity. It is involved in limiting the possible binding orientations of **4** and alters the binding of **1** to nitroreductase compared with its binding to FRase I. Thus, modulating substrate specificity by alteration of the structure of the enzyme rather than the prodrug might usefully focus on modifying this residue and those surrounding it.

Experimental Section

Crystallization and Data Collection. The expression and purification of *E. coli* NTR has been described previously.[22] Yellow, tetragonal crystals that grew to a size of about 0.2 × 0.2 × 0.1 mm were obtained by vapor diffusion at 4 °C from hanging drops of 3 μL equilibrated against varying concentrations of PEG 4000 (25−29%) as the precipitant and 0.1 mM sodium acetate, at pH 4.6. The crystal used to determine the reduced form of the enzyme grew to a size of 0.3 × 0.3 × 0.2 mm. A solution of mother liquor containing excess NADH was prepared, and the crystal was soaked in this for a period of 20 min, after which it was completely discolored. The crystal was then flash-frozen in liquid nitrogen, and data to a maximum resolution of 2.5 Å was collected at the European Synchrotron Radiation Facility (ESRF), Grenoble, beamline BM14.2, on a ADSC Q4 detector with a diamond (111) germanium (220) monochromator, wavelength 0.93 Å.

Solutions of mother liquor, distinct from that used for the reduced form and containing an excess of each of the various prodrugs compounds **2**, **3**, or **4** and the inhibitor **1**, were used to soak native crystals. Data on the crystals with **1**, **2**, or **3** bound were collected to a maximum resolution of 2 Å at the European Synchrotron Radiation Facility (ESRF), Grenoble, beamline BM14.1, on a MAR CCD detector with a germanium 220 monochromator, wavelength 0.93 Å. The data for the complex with compound **4** was collected at the Grenoble beamline BM14.2, on an ADSC Q4 detector with a diamond (111), germanium (220) monochromator, wavelength 0.93 Å to 2.46 Å resolution. Cell dimensions and other crystallographic data are given in Table 2.

Structure Solution and Refinement. Data reduction was carried out with SCALEPACK,[23] and the structures were found to be isomorphous with that of the original native structure. The structures were solved using X-PLOR 3.1[24] by molecular replacement using the structure of the native form of the enzyme (PDB Accession Code 1DS7), including the FMN prosthetic groups. The structures were refined in the space group $P4_12_12$ with unit cell dimensions as shown in Table 1. After several cycles of rigid-body and positional refinement, refinement was continued in CNS[25] and simulated annealing using all data was carried out. Examination of $2F_o - F_c$ and $F_o - F_c$ electron density maps of the reduced crystal structure at this point showed good electron density for the enzyme active sites and revealed that the prosthetic groups deviated from planarity, particularly that of the FMN in Active Site B.

A total of 73 water molecules were gradually added both manually and using the automated CNS script, leading to the final R and R_{free} values of 20.9% and 29.7%.

The residual electron density above the plane of each prosthetic group in the active sites was examined to see if it corresponded to that of the prodrugs (or inhibitor) used in the soaks. The prodrug and inhibitor molecules were constructed using the InsightII[26] modeling package, and the appropriate topology and parameter files were generated in X-PLOR 3.1. The structures were inserted into the electron density and the **2**- and **3**-bound structures were refined with full occupancy for these drugs, whereas compound **4** in its complex was assigned half occupancy. The structures were examined with PROCHECK version 2.2[27] and revealed no significant deviations from established parameters. The atomic coordinates and observed structure factors of each structure have been deposited in the Protein Data Bank.

Compound 2. Electron density corresponding to the prodrug molecules of **2** could be seen in both active sites above the plane of the FMN molecules. Close examination of the electron density maps in the prodrug binding regions, as well as examination of the surrounding amino acid residues and potential bridging solvent molecules, revealed the two molecules of **2** in nonidentical environments in the two active sites. In Active Site A, the prodrug molecule was orientated in such a way that the 2-nitro group was stacked above the plane of the FMN, while in the other cavity the 4-nitro group stacked above the FMN. The average B-factors for the two prodrug molecules were 53.4 Å^2 and 50.8 Å^2 for the drug molecules in Active Sites A and B, respectively. The electron density maps for the prodrug in the active sites are shown in Figure 4. A total of 192 water molecules were gradually added both manually and using the automated CNS script, leading to the final R and R_{free} values of 22.2% and 26.3%.

Compound 3. The regions of electron density corresponding to this prodrug molecule were well defined in both active sites. The orientations of the prodrugs were unequivocal and prodrug fitting into the electron density revealed that they were orientated in such a way that the 2-nitro group was stacked above the plane of the FMN. The average B-factors of the two drug molecules were 52.4 Å^2 and 50.9 Å^2 in Active Sites A and B, respectively. A total of 185 water molecules were included in the same way as for the structure with **2** bound, giving final R and R_{free} values of 23.1% and 28.6%. The electron density maps for the prodrug in the active site are shown in Figure 4.

Compound 4. The resolution of this structure (2.47 Å) was lower than for the previous structures, due to the somewhat weaker beam of Station X compared to that of BM14.1 at the Grenoble Synchrotron. Also, and contrary to the case of the structures with **2** or **3** bound, electron density corresponding to a prodrug molecule was only observed in Active Site B. Fitting the prodrug molecule into this region of density revealed that the orientation was the same as that of compound **3**, and such that the 2-nitro group stacks above the plane of the FMN. The electron density for both the mustard and the amide groups was well defined. The mustard group faces outward from the protein toward Channel A, whereas the amide group faces opposite Channel B toward the ribotide portion of the FMN. A total of 232 water molecules were added to the structure, leading to final R and R_{free} values of 21.4% and 26.4%. The average B-factor for the prodrug was 46.4 Å^2. The electron density maps for the prodrug in the active site are shown in Figure 5d.

Compound 1. A region of density corresponding to the molecule of **1** was only observed above the plane of FMN in Active Site A. One of the hydroxycoumarin subunits was fitted into this region so that it stacked well above the prosthetic group. The electron density for the second hydroxycoumarin subunit was not as well defined as the first, illustrating its ability to adopt alternate conformations. This subunit was therefore given partial occupancy. However, attempts to fit the second portion into alternative regions of density such as into the channel proved unsuccessful. Therefore, and though this portion is probably able to sit in alternate conformations, the positions in which they were refined in this structure appears to correspond to the predominant orientation throughout the crystal lattice. The electron density for the inhibitor is shown in Figure 6c. The final R and R_{free} values were 22.5% and 27.0%, respectively, and the average B-factor for the inhibitor was 51.3 Å^2.

Acknowledgment. This work has been supported by Cancer Research UK (Program Grant SP1384). Most of it was performed at the Chester Beatty Laboratories, The Institute of Cancer Research, when three of us (E.J., G.N.P., and S.N.) were working there. We are also grateful to the Institute of Cancer Research for a studentship to E.J.

References

(1) Rauth, A. M.; Melo, T.; Misra, V. Bioreductive therapies: an overview of drugs and their mechanisms of action. *Int. J. Radiat. Oncol. Biol. Phys.* **1998**, *42*, 755−762.

(2) Niculescu-Duvaz, I.; Friedlos, F.; Niculescu-Duvaz, D.; Davies, L.; Springer, C. J. Prodrugs for antibody- and gene-directed enzyme prodrug therapies (ADEPT and GDEPT). *Anticancer Drug Des.* **1999**, *14*, 517−538.

(3) Zenno, S.; Koike, H.; Tanokura, M.; Saigo, K. Gene cloning, purification, and characterization of NfsB, a minor oxygen-insensitive nitroreductase from *Escherichia coli*, similar in biochemical properties to FRase I, the major flavin reductase in *Vibrio fischeri*. *J Biochem.* (*Tokyo*) **1996**, *120*, 736−744.

(4) Denny, W. A. Nitroreductase-based GDEPT. *Curr. Pharm. Des.* **2002**, *8*, 99−110.

(5) Knox, R. J.; Boland, M. P.; Friedlos, F.; Coles, B.; Southan, C.; Roberts, J. J. The nitroreductase enzyme in Walker cells that activates 5-(aziridin-1-yl)-2,4-dinitrobenzamide (CB 1954) to 5-(aziridin-1-yl)-4-hydroxylamino-2-nitrobenzamide is a form of NAD(P)H dehydrogenase (quinone) (EC 1.6.99.2). *Biochem. Pharmacol.* **1988**, *37*, 4671−4677.

(6) Knox, R.J.; Friedlos, F.; Marchbank, T.; Roberts, J. J. Bioactivation of CB 1954: reaction of the active 4-hydroxylamino derivative with thioesters to form the ultimate DNA-DNA interstrand cross-linking species. *Biochem. Pharmacol.* **1991**, *42*, 1691−1697.

(7) Knox, R. J.; Friedlos, F.; Jarman, M.; Roberts, J. J. A new cytotoxic, DNA interstrand cross-linking agent, 5-(aziridin-1-yl)-4-hydroxylamino-2-nitrobenzamide, is formed from 5-(aziridin-1-yl)-2,4-dinitrobenzamide (CB 1954) by a nitroreductase enzyme in Walker carcinoma cells. *Biochem. Pharmacol.* **1988**, *37*, 4661−4669.

(8) Anlezark, G. M.; Melton, R. G.; Sherwood, R. F.; Coles, B.; Friedlos, F.; Knox, R. J. The bioactivation of 5-(aziridin-1-yl)-2,4-dinitrobenzamide (CB1954)- -I. Purification and properties of a nitroreductase enzyme from *Escherichia coli*- -a potential enzyme for antibody-directed enzyme prodrug therapy (ADEPT). *Biochem. Pharmacol.* **1992**, *44*, 2289−2295.

(9) Westphal, E. M.; Ge, J.; Catchpole, J. R.; Ford, M.; Kenney, S. C. The nitroreductase/CB1954 combination in Epstein−Barr virus-positive B-cell lines: induction of bystander killing in vitro and in vivo. *Cancer Gene Ther.* **2000**, *7*, 97−106.

(10) Chung-Faye, G.; Palmer, C.; Anderson, D.; Clark, J.; Downes, M.; Baddeley, J.; Hussain, S.; Murray, P.I.; Searle, P.; Seymour, L.; Harris, P. A.; Ferry, D.; Kerr, D. J. Virus-directed, enzyme prodrug therapy with nitroimidazole reductase: a phase I and pharmacokinetic study of its prodrug, CB1954. *Clin. Cancer Res.* **2001**, *7*, 2662−2668.

(11) Anlezark, G. M.; Melton, R. G.; Sherwood, R. F.; Wilson, W. R.; Denny, W. A.; Palmer, B. D.; Knox, R. J.; Friedlos, F.; Williams, A. Bioactivation of dinitrobenzamide mustards by an *E. coli* B nitroreductase. *Biochem. Pharmacol.* **1995**, *50*, 609−618.

(12) Palmer, B. D.; Wilson, W. R.; Cliffe, S.; Denny, W. A. Hypoxia-selective antitumor agents. 5. Synthesis of water-soluble nitroaniline mustards with selective cytotoxicity for hypoxic mammalian cells. *J. Med. Chem.* **1992**, *35*, 3214−3222.

(13) Wilson, W. R.; Pullen, S. M.; Hogg, A.; Helsby, N. A.; Hicks, K. O.; Denny, W. A. Quantitation of bystander effects in nitroreductase suicide gene therapy using three-dimensional cell cultures. *Cancer Res.* **2002**, *62*, 1425−1432.

(14) Atwell, G. J.; Boyd, M.; Palmer, B. D.; Anderson, R. F.; Pullen, S. M.; Wilson, W. R.; Denny, W. A. Synthesis and evaluation of 4-substituted analogues of 5-[*N*,*N*-bis(2-chloroethyl)amino]-2-nitrobenzamide as bioreductively activated prodrugs using an *Escherischia coli* nitroreductase. *Anti-Cancer Drug Des.* **1996**, *11*, 553−567.

(15) Friedlos, F.; Denny, W. A.; Palmer, B. D.; Springer, C. J. Mustard prodrugs for activation by *Escherichia coli* nitroreductase in gene-directed enzyme prodrug therapy. *J. Med. Chem.* **1997**, *40*, 1270−1275.

(16) Parkinson, G. N.; Skelly, J. V.; Neidle, S. Crystal structure of FMN-dependent nitroreductase from *Escherichia coli* B: a prodrug-activating enzyme. *J. Med. Chem.* **2000**, *43*, 3624−3631.
(17) Haynes, C. A.; Koder, R. L.; Miller, A. F.; Rodgers, D. W. Structures of nitroreductase in three states: effects of inhibitor binding and reduction. *J. Biol. Chem.* **2002**, *277*, 11513−11520.
(18) Skelly, J. V.; Sanderson, M. R.; Suter, D. A.; Baumann, U.; Read, M. A.; Gregory, D. S.; Bennett, M.; Hobbs, S. M.; Neidle, S. Crystal structure of human DT-diaphorase: a model for interaction with the cytotoxic prodrug 5-(aziridin-1-yl)-2,4-dinitrobenzamide (CB1954). *J. Med. Chem.* **1999**, *42*, 4325−4330.
(19) Koike, H.; Sasaki, H.; Kobori, T.; Zenno, S.; Saigo, K.; Murphy, M. E.; Adman, E. T.; Tanokura, M. 1.8 A crystal structure of the major NAD(P)H: FMN oxidoreductase of a bioluminescent bacterium, *Vibrio fischeri*: overall structure, cofactor and substrate-analogue binding, and comparison with related flavoproteins. *J. Mol. Biol.* **1998**, *280*, 259−273.
(20) Lovering, A. L.; Hyde, E. I.; Searle, P. F.; White, S. A. The structure of *Escherichia coli* nitroreductase complexed with nicotinic acid: three crystal forms at 1.7, 1.8, and 2.4 A resolution. *J. Mol. Biol.* 2001, *309*, 203-213.
(21) Palmer, B. D.; Wilson, W. R.; Anderson, R. F.; Boyd, M.; Denny, W. A. Hypoxia-selective antitumor agents. 14. Synthesis and hypoxic cell cytotoxicity of regioisomers of the hypoxia-selective cytotoxin 5-[*N*,*N*-bis(2-chloroethyl)amino]-2,4-dinitrobenzamide. *J. Med Chem* **1996**, *39*, 2518−2528.
(22) Skelly, J. V.; Collins, P. J.; Knox, R. J.; Anlezark, G. M.; Melton, R. G. Crystallization and preliminary crystallographic data for an FMN-dependent nitroreductase from *Escherichia coli* B. *J. Mol. Biol.* **1994**, *238*, 852−853.
(23) Otwinowski, Z.; Minor, W. *Data Collection and Processing*; SERC Daresbury Laboratory: Warrington, UK, 1993.
(24) Brünger, A. T. Free R Value: a novel quantity for assessing the accuracy of crystal structures. *Nature* **1992**, *355*, 472−475.
(25) Brünger, A. T; Adams, P. D.; Clore, G. M.; DeLano, W. L.; Gros, P.; Grosse-Kunstleve, R. W.; Jiang, J.-S.; Kuszewski, J.; Nilges, M.; Pannu, N. S.; Read, R. J.; Rice, L. M.; Simonson, T.; Warren, G. L. Crystallography & NMR system: A new software suite for macromolecular structure determination. *Acta Crystallogr.* **1998**, D*54*, 905−921.
(26) MSI 1997. INSIGHTII Molecular modelling environment (San Deigo).
(27) Laskowski, R. A.; MacArther, M. W.; Moss, D. S.; Thornton, J. M. PROCHECK: A program to check the sterochemical quality of protein structures. *J. Appl. Crystallogr.* **1993**, *26*, 283−291.

JM030843B